# Adaptive Spacecraft Attitude Tracking Control with Actuator Uncertainties

Hyungjoo Yoon* and Panagiotis Tsiotras†
*Georgia Institute of Technology*
*Atlanta, Georgia 30332-0150, USA*

**An adaptive control algorithm for the spacecraft attitude tracking problem for the case when the spin axis directions of the flywheel actuators are uncertain is developed. The spacecraft equations of motion in this case are fully nonlinear and can be represented as a Multi-Input-Multi-Output (MIMO) system. Adaptive tracking control is therefore challenging for this problem. In this paper the second-order equation of motion of the spacecraft plus the actuators is initially converted to a first-order state space form, and subsequently an adaptive controller is designed based on Lyapunov stability theory. A smooth projection algorithm is then applied to keep the parameter estimates inside a singularity-free region. The controller successfully deals with unknown misalignments of the axis directions of the flywheel actuators. It is noted that the proposed design procedure can also be easily applied to more general MIMO dynamical systems.**

## I. Introduction

Adaptive attitude control of a spacecraft with uncertain parameters has been studied intensively in the past decade.[1–8] However, most (if not all) of the previous research work deals only with uncertainties in the inertia matrix of the spacecraft, assuming that an exact model of the actuators is available. In other words, these results have been derived under the implicit assumption that the torque axis directions and/or input scalings of the actuators (such as gas jets, reaction wheels, or CMGs/VSCMGs etc.) are exactly known. This assumption is rarely satisfied in practice because of misalignment of the actuators during installation, due to aging and wearing out of the mechanical and electrical parts, etc. For most cases the effect of these uncertainties on the overall system performance is not significant. However, for the case of flywheels used as "mechanical batteries" in a Integrated Power and Attitude Control System (IPACS)[8–10] even small misalignments of the flywheel axes can be detrimental. Flywheels for IPACS applications spin at very high speeds and have large amounts of stored kinetic energy (and hence angular momentum). Precise attitude control requires proper momentum management, while not generating large spurious output torques. This can be achieved with the use of at least four flywheels (in the simplest scenario) whose angular momenta have to be canceled or regulated with high precision. If the exact direction of the axes of the flywheels (hence the angular momenta) are not known with sufficient accuracy, large output torque errors will impart the attitude of the spacecraft.

One of the main difficulties encountered when designing adaptive controllers dealing with actuator uncertainties is the Multi-Input-Multi-Output (MIMO) form of the spacecraft equations of motion. The controller has to track at least three attitude parameters (for full three-axis attitude control). Complete control therefore requires, in general, three or more actuator torques. A lot of research has been devoted to the adaptive tracking problem. Most previous results in this area deal only with the Single-Input-Single-Output (SISO) or uncoupled multi-input case. Slotine et al.[1,11] proposed adaptive controllers for MIMO systems, but these

*Currently with Samsung Electronics Co., Korea. Email: drake.yoon@gmail.com. Tel: +82-10-2313-1097.
†Professor, School of Aerospace Engineering. Email: p.tsiotras@ae.gatech.edu. Tel: +1-404-894-9526. Fax: +1-404-894-2760. Associate Fellow AIAA. Corresponding author.

systems must be Hamiltonian, and the uncertainties should appear in the inertia and/or Coriolis/centrifugal terms, but not in the actuators. Ge[12] derived an adaptive control law for multi-link robot manipulator systems with uncertainties in the control input term, but the uncertainty must be in the input scalings. That is, the uncertainty matrix is diagonal if it is represented in multiplicative form.

Recently, Chang[13] provided an adaptive, robust tracking control algorithm for nonlinear MIMO systems. His work is based on the "smooth projection algorithm," which has also been used in Refs. 14 and 15 for adaptive control of SISO systems. This algorithm plays a key role in our developments and keeps the parameter estimates inside a properly defined convex set, so that the estimates do not drift into a region where the control law may become singular. By "singularity" here we mean actuator configurations for which the control logic commands have very large values.

In this article, an adaptive control law is designed for spacecraft attitude tracking using Variable Speed Control Moment Gyros (VSCMGs),[8,10,16] whose gimbal axis directions are not exactly known. A VSCMG is a spacecraft attitude actuator, which has been recently introduced as an alternative to conventional control moment gyros (CMGs) and reaction wheels (RWs). It seems to be especially suitable for IPACS applications (since the attitude control and the energy storage functions can be "decoupled"[8]), as well as for developing singularity-free steering laws in lieu of standard CMGs.[16] A VSCMG generates a torque by exchanging angular momentum (both in magnitude and direction) with the spacecraft body. As its name implies, a VSCMG is essentially a single-gimbal control moment gyro (CMG), where the flywheel is allowed to have variable speed. A VSCMG is therefore a hybrid device that combines the capabilities of a conventional single-gimbal CMG and a reaction wheel.

The equations of motion of a spacecraft with a cluster of VSCMGs are rather complicated.[8,10,17] Thus, in this paper a set of simplified equations will be used to assist with the control law design. The final controller will nonetheless be validated against the complete, nonlinear model.

Even though the baseline control design is provided for a spacecraft with VSCMGs, it can be easily generalized and applied to other dynamical systems, whose equations of motion can be written in the standard second-order vector form, for instance, a spacecraft controlled by means of other types of actuators or multi-link robot manipulators.

## II. Problem Statement

Consider a spacecraft with a VSCMG cluster containing $N$ flywheels, as shown in Figure 1.

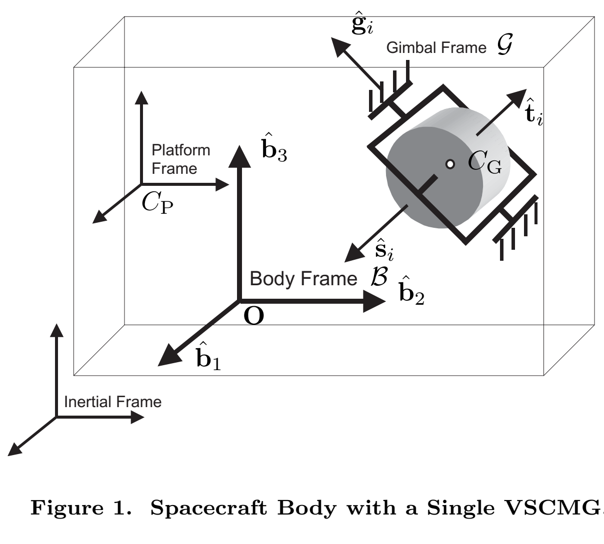


**Figure 1. Spacecraft Body with a Single VSCMG.**

The definition of the axes in Figure 1 are as follows ($i = 1, \ldots, N$).

- $\hat{\mathbf{g}}_i$ : VSCMG gimbal axis unit vector
- $\hat{\mathbf{s}}_i$ : VSCMG spin axis unit vector
- $\hat{\mathbf{t}}_i$ : VSCMG transverse axis unit vector (torque vector) given as $\hat{\mathbf{t}}_i = \hat{\mathbf{g}}_i \times \hat{\mathbf{s}}_i$.

With a slight abuse of notation, in the sequel we will use boldface symbols to denote both a vector and its representation in a standard basis. This simplification should not cause any problems, as the meaning of the expression (and the basis used) should be clear from the context. If we need to refer to a representation with respect to a specific frame, we will use subscripts to denote the frame used.

The dynamic equations of motion of the spacecraft can be written as[8]

$$\dot{J}\boldsymbol{\omega} + J\dot{\boldsymbol{\omega}} + A_{\mathrm{g}} I_{\mathrm{cg}} \ddot{\boldsymbol{\gamma}} + A_{\mathrm{t}} I_{\mathrm{ws}} [\boldsymbol{\Omega}]^{d} \dot{\boldsymbol{\gamma}} + A_{\mathrm{s}} I_{\mathrm{ws}} \dot{\boldsymbol{\Omega}} + \boldsymbol{\omega}^{\times}\Big( J\boldsymbol{\omega} + A_{\mathrm{g}} I_{\mathrm{cg}} \dot{\boldsymbol{\gamma}} + A_{\mathrm{s}} I_{\mathrm{ws}} \boldsymbol{\Omega} \Big) = 0, \tag{1}$$

where $J = {}^{B}I + A_{\mathrm{s}} I_{cs} A_{\mathrm{s}}^{T} + A_{\mathrm{t}} I_{\mathrm{ct}} A_{\mathrm{t}}^{T} + A_{\mathrm{g}} I_{\mathrm{cg}} A_{\mathrm{g}}^{T}$ is the total moment of inertia of the spacecraft, $\boldsymbol{\omega}$ is the body rate vector of the spacecraft, and $\boldsymbol{\gamma} = (\gamma_1, \ldots, \gamma_N)^T \in \mathbb{R}^N$ and $\boldsymbol{\Omega} = (\Omega_1, \ldots, \Omega_N)^T \in \mathbb{R}^N$ are column vectors, whose elements are the gimbal angles and the wheel speeds of the VSCMGs with respect to the gimbals, respectively. The matrices $A_\star \in \mathbb{R}^{3\times N}$ have as columns the gimbal, spin and transverse directional unit vectors expressed in the body-frame, where $\star$ is $\mathrm{g}, \mathrm{s}$ or $\mathrm{t}$. They depend on the gimbal angles as follows

$$A_{\mathrm{g}} = A_{\mathrm{g}0} \tag{2}$$

$$A_{\mathrm{s}} = A_{\mathrm{s}0}[\cos\gamma]^{d} + A_{\mathrm{t}0}[\sin\gamma]^{d} \tag{3}$$

$$A_{\mathrm{t}} = A_{\mathrm{t}0}[\cos\gamma]^{d} - A_{\mathrm{s}0}[\sin\gamma]^{d} \tag{4}$$

The matrices $I_{\mathrm{c}\star}$ and $I_{\mathrm{w}\star}$ are diagonal with elements the values of the inertias of the gimbal plus wheel structure and wheel-only-structure of the VSCMGs, respectively. The skew-symmetric matrix $\boldsymbol{v}^{\times}$, for $\boldsymbol{v} \in \mathbb{R}^3$, represents the cross product operation. See Refs. 8 and 18 for the details in deriving (1).

In general, the total moment of inertia of the spacecraft will change as the VSCMG rotates about its gimbal axis, so the matrix $J$ is a function of a gimbal angle $\gamma$, that is, $J = J(\gamma)$. However, this dependence of $J$ on $\gamma$ is weak, especially when the size of spacecraft main body is large. We will therefore assume that $J$ is constant ($\dot{J} = 0$) during controller design. In addition, to simplify the analysis, the gimbal acceleration term $A_{\mathrm{g}} I_{\mathrm{cg}} \ddot{\boldsymbol{\gamma}}$ will be ignored. This assumption is standard in the literature,[16,19,20] and essentially amounts to gimbal angle rate servo control. It is also useful to assume that the gimbal angle rate term $A_{\mathrm{g}} I_{\mathrm{cg}} \dot{\boldsymbol{\gamma}}$ does not contribute significantly to the total angular momentum. One then obtains the simplified equation of motion as

$$J\dot{\boldsymbol{\omega}} + C(\boldsymbol{\gamma}, \boldsymbol{\Omega})\dot{\boldsymbol{\gamma}} + D(\boldsymbol{\gamma})\dot{\boldsymbol{\Omega}} + \boldsymbol{\omega}^{\times}\mathbf{h} = 0, \tag{5}$$

where,

$$\mathbf{h} = J\boldsymbol{\omega} + A_{\mathrm{s}} I_{\mathrm{ws}} \boldsymbol{\Omega}, \tag{6}$$

is the total angular momentum of the spacecraft and VSCMG system, and where,

$$C(\boldsymbol{\gamma}, \boldsymbol{\Omega}) = A_{\mathrm{t}} I_{\mathrm{ws}} \boldsymbol{\Omega}^{d}, \quad D(\boldsymbol{\gamma}) = A_{\mathrm{s}} I_{\mathrm{ws}}. \tag{7}$$

Notice that this equation has been derived for a spacecraft with a VSCMG cluster, and therefore it subsumes the reaction wheel case (by setting $\boldsymbol{\gamma}$ to be constant to the above equations), and the conventional CMG case (by setting $\boldsymbol{\Omega}$ to be constant).

The modified Rodrigues parameters[21–23] (MRPs) are chosen to describe the attitude kinematics of the spacecraft. The MRPs are defined in terms of the Euler principal unit vector $\hat{\boldsymbol{\eta}}$ and angle $\phi$ by $\boldsymbol{\sigma} = \hat{\boldsymbol{\eta}} \tan(\phi/4)$. The MRPs have the advantage of being well defined for the whole range for rotations,[21,22,24] i.e., $\phi \in [0, 2\pi)$. The differential equation that governs the kinematics in terms of the MRPs is given by

$$\dot{\boldsymbol{\sigma}} = G(\boldsymbol{\sigma})\boldsymbol{\omega} \tag{8}$$

where $G(\boldsymbol{\sigma}) = \frac{1}{2}\Big(\mathbf{I} + [\boldsymbol{\sigma}^{\times}] + \boldsymbol{\sigma}\boldsymbol{\sigma}^{T} - [\frac{1}{2}(1 + \boldsymbol{\sigma}^{T}\boldsymbol{\sigma})]\,\mathbf{I}\Big)$ and $\mathbf{I}$ is the $3\times 3$ identity matrix. We hasten to point out that the use of the MRPs to describe the kinematics is done without loss of generality. Any other suitable kinematic description could have been used with the conclusions of the paper remaining essentially the same.

From Eq. (8), one obtains $\boldsymbol{\omega} = G^{-1}(\boldsymbol{\sigma})\dot{\boldsymbol{\sigma}}$ and $\ddot{\boldsymbol{\sigma}} = G(\boldsymbol{\sigma})\dot{\boldsymbol{\omega}} + \dot{G}(\boldsymbol{\sigma}, \dot{\boldsymbol{\sigma}})\,\boldsymbol{\omega}$. The total angular momentum $\mathbf{h}$, written in the body frame can be expressed as $\mathbf{h} = R_{\mathcal{I}}^{\mathcal{B}}(\boldsymbol{\sigma})\mathbf{H}_{\mathcal{I}}$, where $R_{\mathcal{I}}^{\mathcal{B}}(\boldsymbol{\sigma})$ is the rotational matrix from the inertial frame $\mathcal{I}$ to the body frame $\mathcal{B}$, and $\mathbf{H}_{\mathcal{I}}$ is the total angular momentum written in the $\mathcal{I}$-frame. If we assume that no external control/disturbance torques act on the spacecraft, then the total angular momentum of the spacecraft-VSCMG system is conserved (in both magnitude and direction) during a maneuver, and thus $\mathbf{H}_{\mathcal{I}}$ is constant. From, Eq. (5), one can then write

$$G^{-T} J G^{-1} \ddot{\boldsymbol{\sigma}} - G^{-T} J G^{-1} \dot{G} G^{-1} \dot{\boldsymbol{\sigma}} + G^{-T} \boldsymbol{\omega}^{\times} (R_{\mathcal{I}}^{\mathcal{B}}(\boldsymbol{\sigma}) \mathbf{H}_{\mathcal{I}}) + G^{-T} (C\dot{\boldsymbol{\gamma}} + D\dot{\boldsymbol{\Omega}}) = 0, \tag{9}$$

equivalently,

$$\ddot{\boldsymbol{\sigma}} = F^*(\boldsymbol{\sigma}, \dot{\boldsymbol{\sigma}}) + G^*(\boldsymbol{\sigma}, \dot{\boldsymbol{\sigma}})\boldsymbol{u}, \tag{10}$$

where,

$$F^*(\boldsymbol{\sigma}, \dot{\boldsymbol{\sigma}}) = {H^*}^{-1}\left(G^{-T}JG^{-1}\dot{G}G^{-1}\dot{\boldsymbol{\sigma}} - G^{-T}\boldsymbol{\omega}^\times(R^{\mathcal{B}}_{\mathcal{I}}(\boldsymbol{\sigma})\mathbf{H}_{\mathcal{I}})\right), \tag{11a}$$

$$G^*(\boldsymbol{\sigma}, \boldsymbol{\gamma}, \boldsymbol{\Omega}) = -{H^*}^{-1}G^{-T}Q, \tag{11b}$$

$$H^*(\boldsymbol{\sigma}) = G^{-T}JG^{-1}, \tag{11c}$$

$$Q(\boldsymbol{\gamma}, \boldsymbol{\Omega}) = [C(\boldsymbol{\gamma}, \boldsymbol{\Omega})\ ,\ D(\boldsymbol{\gamma})], \tag{11d}$$

with control input vector,

$$\boldsymbol{u} = [\dot{\boldsymbol{\gamma}}^T, \dot{\boldsymbol{\Omega}}^T]^T \in \mathbb{R}^{2N\times 1}. \tag{12}$$

Therefore, the equation of motion in state-space form can be written as

$$\frac{\mathrm{d}}{\mathrm{d}t}\begin{bmatrix}\boldsymbol{\sigma}\\ \dot{\boldsymbol{\sigma}}\end{bmatrix} = \begin{bmatrix}0 & \mathbf{I}\\ 0 & 0\end{bmatrix}\begin{bmatrix}\boldsymbol{\sigma}\\ \dot{\boldsymbol{\sigma}}\end{bmatrix} + \begin{bmatrix}0\\ \mathbf{I}\end{bmatrix}\Big(F^*(\boldsymbol{\sigma}, \dot{\boldsymbol{\sigma}}) + G^*(\boldsymbol{\sigma}, \dot{\boldsymbol{\sigma}})\boldsymbol{u}\Big). \tag{13}$$

Suppose now that there are uncertainties in the modelling of the actuators, so that the exact values of the initial/reference axis directions and scaling input gains are unknown. Let us assume that the actual initial axis direction matrices of the wheels can be expressed as

$$A_{s0} = A^{\mathrm{n}}_{s0} + A^{\Delta}_{s0}, \quad A_{t0} = A^{\mathrm{n}}_{t0} + A^{\Delta}_{t0} \tag{14}$$

where $A^{\mathrm{n}}_{\bullet 0}$ are known nominal values and $A^{\Delta}_{\bullet 0}$ are unknown constant values of the matrices $A_{s0}$ and $A_{t0}$. Moreover, since we do not know the exact angular momentum of the VSCMG cluster, the total angular momentum $\mathbf{H}_{\mathcal{I}}$ can be expressed as

$$\mathbf{H}_{\mathcal{I}} = \mathbf{H}^{\mathrm{n}}_{\mathcal{I}} + \mathbf{H}^{\Delta}_{\mathcal{I}} \tag{15}$$

where $\mathbf{H}^{\mathrm{n}}_{\mathcal{I}}$ is the known nominal value of $\mathbf{H}_{\mathcal{I}}$ in the inertial frame, and $\mathbf{H}^{\Delta}_{\mathcal{I}}$ is an unknown constant vector. Dropping the arguments for convenience, the system matrices in (11a) and (11b) can be decomposed as

$$F^* = F^{*\mathrm{n}} + F^{*\Delta}, \quad G^* = G^{*\mathrm{n}} + G^{*\Delta} \tag{16}$$

where,

$$F^{*\mathrm{n}} = {H^*}^{-1}\left(G^{-T}JG^{-1}\dot{G}G^{-1}\dot{\boldsymbol{\sigma}} - G^{-T}\boldsymbol{\omega}^\times(R^{\mathcal{B}}_{\mathcal{I}}(\boldsymbol{\sigma})\mathbf{H}^{\mathrm{n}}_{\mathcal{I}})\right), \tag{17}$$

$$F^{*\Delta} = -{H^*}^{-1}\left(G^{-T}\boldsymbol{\omega}^\times(R^{\mathcal{B}}_{\mathcal{I}}(\boldsymbol{\sigma})\mathbf{H}^{\Delta}_{\mathcal{I}})\right), \tag{18}$$

and

$$G^{*\mathrm{n}} = -{H^*}^{-1}G^{-T}Q^{\mathrm{n}}, \tag{19}$$

$$G^{*\Delta} = -{H^*}^{-1}G^{-T}Q^{\Delta}, \tag{20}$$

where $Q^{\mathrm{n}}$ and $Q^{\Delta}$ are the nominal and uncertain values of the matrix $Q$ in Eq. (11d), respectively.

Notice that $F^{*\Delta}$ is linear in the uncertain elements of the vector $\mathbf{H}^{\Delta}_{\mathcal{I}}$, thus it can be written as

$$F^{*\Delta} = Y_F\Theta_F \tag{21}$$

where $\Theta_F = \mathbf{H}^{\Delta}_{\mathcal{I}}$. The matrix $Y_F$ is the "regressor matrix," and can be constructed from the measurements of $\boldsymbol{\sigma}$ and $\dot{\boldsymbol{\sigma}}$. In addition, $G^{*\Delta}$ can be written similarly as

$$G^{*\Delta} = Y_G\Theta_G, \tag{22}$$

where $\Theta_G$ is a $12N \times 2N$ matrix defined by

$$\Theta_G = \mathrm{diag}[\Theta_{G1}, \Theta_{G2}, \cdots, \Theta_{G2N}], \tag{23}$$

$$\Theta_{Gi} = \Theta_{G(i+N)} = [{\mathbf{t}^{\Delta}_{i0}}^T, {\mathbf{s}^{\Delta}_{i0}}^T]^T \in \mathbb{R}^{6\times 1}, \qquad i = 1, \cdots, N, \tag{24}$$

and $Y_G$ is a $3 \times 12N$ matrix defined by

$$Y_G = [Y_{G1}, Y_{G2}, \cdots, Y_{G2N}], \tag{25}$$

where,

$$Y_{Gi} = -{H^*}^{-1} G^{-T} I_{\text{cg}} [\mathbf{I}_3 \cos\gamma_i,\ -\mathbf{I}_3 \sin\gamma_i] \in \mathbb{R}^{3\times 6}, \quad i = 1, \cdots, N, \tag{26}$$

$$Y_{Gi} = -{H^*}^{-1} G^{-T} I_{\text{cg}} [\mathbf{I}_3 \sin\gamma_i,\ \mathbf{I}_3 \cos\gamma_i] \in \mathbb{R}^{3\times 6}, \quad i = N+1, \cdots, 2N. \tag{27}$$

## III. Adaptive Controller Design

Assume that the attitude to be tracked is given in terms of some known functions $\boldsymbol{\sigma}_d(t)$, $\dot{\boldsymbol{\sigma}}_d(t)$ and $\ddot{\boldsymbol{\sigma}}_d(t)$ for $t \geq 0$. Here $\boldsymbol{\sigma}_d$ is the MRP vector presenting the attitude of a desired reference frame ($\mathcal{D}$-frame) with respect to the inertial frame ($\mathcal{I}$-frame). Defining the error

$$\mathbf{e} \triangleq \begin{bmatrix} \boldsymbol{\sigma}_e \\ \dot{\boldsymbol{\sigma}}_e \end{bmatrix} = \begin{bmatrix} \boldsymbol{\sigma} - \boldsymbol{\sigma}_d \\ \dot{\boldsymbol{\sigma}} - \dot{\boldsymbol{\sigma}}_d \end{bmatrix}, \tag{28}$$

one obtains the tracking error dynamics from Eq. (13) as

$$\dot{\mathbf{e}} = A_0 \mathbf{e} + B\left(F^*(\boldsymbol{\sigma}, \dot{\boldsymbol{\sigma}}) + G^*(\boldsymbol{\sigma}, \dot{\boldsymbol{\sigma}})\boldsymbol{u} - \ddot{\boldsymbol{\sigma}}_d\right), \tag{29}$$

where

$$A_0 \triangleq \begin{bmatrix} 0 & \mathbf{I} \\ 0 & 0 \end{bmatrix}, \qquad B \triangleq \begin{bmatrix} 0 \\ \mathbf{I} \end{bmatrix}. \tag{30}$$

It can be easily shown that the pair $(A_0, B)$ is controllable, so one can choose a gain matrix $K$ such that $A \triangleq A_0 - BK$ is Hurwitz, and rewrite (29) as

$$\dot{\mathbf{e}} = A\mathbf{e} + B\left(K\mathbf{e} + F^*(\boldsymbol{\sigma}, \dot{\boldsymbol{\sigma}}) + G^*(\boldsymbol{\sigma}, \dot{\boldsymbol{\sigma}})\boldsymbol{u} - \ddot{\boldsymbol{\sigma}}_d\right) \tag{31}$$

Let now $P = P^T > 0$ be a solution to the Lyapunov equation

$$A^T P + PA + R = 0, \qquad R = R^T > 0, \tag{32}$$

and choose a Lyapunov function as

$$V = \frac{1}{2}\mathbf{e}^T P \mathbf{e} + \frac{1}{2\alpha_F}\tilde{\Theta}_F^T \tilde{\Theta}_F + \frac{1}{2\alpha_G}\text{Tr}(\tilde{\Theta}_G^T \tilde{\Theta}_G), \quad \alpha_F, \alpha_G > 0, \tag{33}$$

where $\tilde{\Theta}_\bullet \triangleq \hat{\Theta}_\bullet - \Theta_\bullet$, and $\hat{\Theta}_\bullet$ is an estimate of $\Theta_\bullet$ to be determined by the parameter adaptation law.

Since the dynamics $\dot{\mathbf{e}} = A\mathbf{e}$ is asymptotically stable, if the matrices $F^*(\boldsymbol{\sigma}, \dot{\boldsymbol{\sigma}})$ and $G^*(\boldsymbol{\sigma}, \dot{\boldsymbol{\sigma}})$ were completely known we could choose $u$ to cancel the extra terms in (31), that is,

$$G^*(\boldsymbol{\sigma}, \dot{\boldsymbol{\sigma}})\boldsymbol{u} + K\mathbf{e} + F^*(\boldsymbol{\sigma}, \dot{\boldsymbol{\sigma}}) - \ddot{\boldsymbol{\sigma}}_d = 0. \tag{34}$$

Since $F^*(\boldsymbol{\sigma}, \dot{\boldsymbol{\sigma}})$ and $G^*(\boldsymbol{\sigma}, \dot{\boldsymbol{\sigma}})$ are not known, we will use (16) and replace (34) with its best estimate, that is,

$$(G^{*\text{n}} + Y_G \hat{\Theta}_G)\boldsymbol{u} + K\mathbf{e} + (F^{*\text{n}} + Y_F \hat{\Theta}_F) - \ddot{\boldsymbol{\sigma}}_d = 0. \tag{35}$$

Assuming we have at least two wheels ($N \geq 2$), the solution to (35) exists as long as the $3 \times 2N$ matrix $(G^{*\text{n}} + Y_G \hat{\Theta}_G)$ has full row rank. In this case, the minimum norm solution is given by

$$\boldsymbol{u} = (G^{*\text{n}} + Y_G \hat{\Theta}_G)^\dagger (-K\mathbf{e} - F^{*\text{n}} - Y_F \hat{\Theta}_F + \ddot{\boldsymbol{\sigma}}_d), \tag{36}$$

where $(\bullet)^\dagger$ denotes the pseudo-inverse of a matrix. The tracking error dynamics with the control law (36) reduces to

$$\begin{aligned} \dot{\mathbf{e}} &= A\mathbf{e} + B\Big(K\mathbf{e} + F^{*\text{n}} + Y_F \Theta_F + (G^{*\text{n}} + Y_G \hat{\Theta}_G - Y_G \tilde{\Theta}_G)\boldsymbol{u} - \ddot{\boldsymbol{\sigma}}_d\Big) \\ &= A\mathbf{e} + BK\mathbf{e} + BF^{*\text{n}} + BY_F(\hat{\Theta}_F - \tilde{\Theta}_F) \\ &\quad + B(-K\mathbf{e} - F^{*\text{n}} - Y_F \hat{\Theta}_F + \ddot{\boldsymbol{\sigma}}_d) - BY_G \tilde{\Theta}_G \boldsymbol{u} - B\ddot{\boldsymbol{\sigma}}_d \\ &= A\mathbf{e} - BY_F \tilde{\Theta}_F - BY_G \tilde{\Theta}_G \boldsymbol{u}. \end{aligned} \tag{37}$$

The time derivative of $V$ then becomes

$$\begin{aligned}\dot{V} &= \tfrac{1}{2}\mathbf{e}^T(A^TP+PA)\mathbf{e} - \mathbf{e}^TPBY_F\tilde{\Theta}_F - \mathbf{e}^TPBY_G\tilde{\Theta}_G\boldsymbol{u} \\ &\quad + \frac{1}{\alpha_F}\dot{\hat{\Theta}}_F\tilde{\Theta}_F + \frac{1}{\alpha_G}\mathrm{Tr}(\dot{\hat{\Theta}}_G\tilde{\Theta}_G) \\ &= -\tfrac{1}{2}\mathbf{e}^TR\mathbf{e} + \tfrac{1}{\alpha_F}\tilde{\Theta}_F^T(\dot{\hat{\Theta}}_F - \alpha_FY_F^TB^TP\mathbf{e}) + \tfrac{1}{\alpha_G}\mathrm{Tr}[\tilde{\Theta}_G^T(\dot{\hat{\Theta}}_G - \alpha_GY_G^TB^TP\mathbf{e}\boldsymbol{u}^T)] \\ &= -\tfrac{1}{2}\mathbf{e}^TR\mathbf{e} + \tfrac{1}{\alpha_F}\tilde{\Theta}_F^T(\dot{\hat{\Theta}}_F - \alpha_FY_F^TB^TP\mathbf{e}) + \textstyle\sum_{i=1}^{2N}\tilde{\Theta}_{Gi}^T(\dot{\hat{\Theta}}_{Gi} - \alpha_GY_{Gi}^TB^TP\mathbf{e}\boldsymbol{u}_i).\end{aligned} \tag{38}$$

Choosing the parameter adaptation law

$$\dot{\hat{\Theta}}_F = \alpha_FY_F^TB^TP\mathbf{e}, \tag{39}$$

$$\dot{\hat{\Theta}}_{Gi} = \alpha_GY_{Gi}^TB^TP\mathbf{e}\boldsymbol{u}_i, \quad i=1,\cdots,2N. \tag{40}$$

results in $\dot{V} = -\frac{1}{2}\mathbf{e}^TR\mathbf{e} < 0$. It follows that $\mathbf{e}\to 0$ as $t\to\infty$.

### A. Parameter Projection

A drawback of the previous adaptation law is that the estimate of the parameter $\hat{\Theta}_G$ can result in $(G^{*\mathrm{n}} + Y_G\hat{\Theta}_G)$ losing rank. If we use more than two VSCMGs with their nominal gimbal axes not parallel to each other,[16] the nominal matrix $G^{*\mathrm{n}}$ has necessarily full row rank. Therefore, if the true value of the parameter uncertainty $\Theta_G$ is bounded by a sufficiently small number, and we can also keep its estimated value $\hat{\Theta}_G$ small, then we can expect that $G^{*\mathrm{n}} + Y_G\hat{\Theta}_G$ will also be full row rank. To this end, we make the following two assumptions.

- **Assumption 1.** The actual value $\Theta_{Gi}$ belongs to the set $\Omega_{\Theta_{Gi}} = \left\{\Theta_{Gi}\in\mathbb{R}^6 \mid \|\Theta_{Gi}\|^2 < \beta_{Gi}\right\}$, where $\beta_{Gi} > 0$ is known.
- **Assumption 2.** Let the set $\hat{\Omega}_{\Theta_{Gi}} = \left\{\hat{\Theta}_{Gi}\in\mathbb{R}^6 \mid \|\hat{\Theta}_{Gi}\|^2 < \beta_{Gi}+\delta_{Gi},\ \delta_{Gi}>0\right\}$. The set $\hat{\Omega}_{\Theta_{Gi}}$ contains $\Omega_{\Theta_{Gi}}$ in its interior. If $\hat{\Theta}_{Gi}\in\hat{\Omega}_{\Theta_{Gi}}$ for all $i=1,\cdots,2N$, then $(G^{*\mathrm{n}} + Y_G\hat{\Theta}_G)$ is non-singular.

Now, instead of the adaptation law (40), one can use the "smooth projection algorithm"[13–15]

$$\dot{\hat{\Theta}}_{Gi} = \mathrm{Proj}(\hat{\Theta}_{Gi}, \Phi_{Gi}), \qquad i=1,\cdots,2N, \tag{41}$$

where

$$\Phi_{Gi} \triangleq Y_{Gi}^TB^TP\mathbf{e}\boldsymbol{u}_i, \tag{42}$$

and

$$\mathrm{Proj}(\hat{\Theta}_{Gi},\Phi_{Gi}) = \begin{cases} \alpha_G\Phi_{Gi}, & \text{if (i) } \|\hat{\Theta}_{Gi}\|^2 < \beta_{Gi}\ , \\ & \text{or } \|\hat{\Theta}_{Gi}\|^2 \geq \beta_{Gi} \text{ and } \Phi_{Gi}^T\hat{\Theta}_{Gi} \leq 0, \\ \alpha_G\left(\Phi_{Gi} - \frac{(\|\hat{\Theta}_{Gi}\|^2-\beta_{Gi})\Phi_{Gi}^T\hat{\Theta}_{Gi}}{\delta_{Gi}\|\hat{\Theta}_{Gi}\|^2}\hat{\Theta}_{Gi}\right) & \\ & \text{if (ii) } \|\hat{\Theta}_{Gi}\|^2 \geq \beta_{Gi} \text{ and } \Phi_{Gi}^T\hat{\Theta}_{Gi} > 0. \end{cases} \tag{43}$$

This adaptation law is identical to (40) in case (i), and switches smoothly to another expression in case (ii). The projection operator $\mathrm{Proj}(\hat{\Theta}_{Gi},\Phi_{Gi})$ is locally Lipschitz in $(\hat{\Theta}_{Gi},\Phi_{Gi})$, thus the system has a unique solution defined for some time interval $[0,T)$, $T>0$. It can be verified that the adaptation rule (41)-(43) satisfies

$$\tilde{\Theta}_{Gi}^T(\dot{\hat{\Theta}}_{Gi} - \alpha_G\Phi_{Gi}) \leq 0. \tag{44}$$

As a result,

$$\hat{\Theta}_{Gi}(t=0)\in\Omega_{\Theta_{Gi}} \Rightarrow \hat{\Theta}_{Gi}(t)\in\hat{\Omega}_{\Theta_{Gi}}, \quad \forall t\geq 0. \tag{45}$$

The proof of this statement can be seen as follows. In case (i) the equality in Eq. (44) trivially holds, and $\dot{\hat{\Theta}}_{Gi}^T\hat{\Theta}_{Gi} = \alpha_G\Phi_{Gi}^T\hat{\Theta}_{Gi} \leq 0$, thus the estimate $\hat{\Theta}_{Gi}$ moves closer to zero. In case (ii), the left hand side of Eq. (44) becomes

$$\tilde{\Theta}_{Gi}^T(\dot{\hat{\Theta}}_{Gi} - \alpha_G\Phi_{Gi}) = -\alpha_G\frac{(\|\hat{\Theta}_{Gi}\|^2 - \beta_{Gi})\Phi_{Gi}^T\hat{\Theta}_{Gi}}{\delta_{Gi}\|\hat{\Theta}_{Gi}\|^2}\tilde{\Theta}_{Gi}^T\hat{\Theta}_{Gi} \ \leq \ 0, \tag{46}$$

because $\tilde{\Theta}_{Gi}^T\hat{\Theta}_{Gi} \geq 0$ as shown in Figure 2. On the other hand,

$$\dot{\hat{\Theta}}_{Gi}^T\hat{\Theta}_{Gi} = \alpha_G\Phi_{Gi}^T\hat{\Theta}_{Gi}\left(1 - \frac{(\|\hat{\Theta}_{Gi}\|^2 - \beta_{Gi})}{\delta_{Gi}}\right)\begin{cases} < 0 & \text{if } \|\hat{\Theta}_{Gi}\|^2 > \beta_{Gi} + \delta_{Gi}, \\ = 0 & \text{if } \|\hat{\Theta}_{Gi}\|^2 = \beta_{Gi} + \delta_{Gi}, \\ > 0 & \text{if } \|\hat{\Theta}_{Gi}\|^2 < \beta_{Gi} + \delta_{Gi}, \end{cases} \tag{47}$$

thus $\hat{\Theta}_{Gi}$ does not drift outward the set $\hat{\Omega}_{\Theta_{Gi}}$.

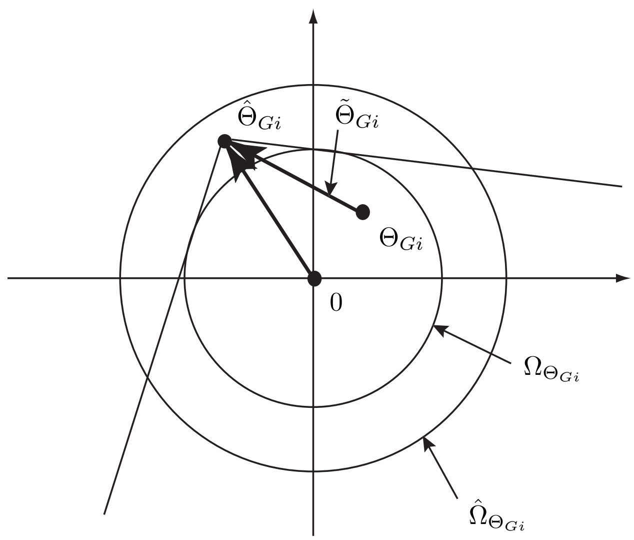


**Figure 2.** $\tilde{\Theta}_{Gi}^T\hat{\Theta}_{Gi} \geq 0$ **in Case (ii).**

From the above observations, one concludes that using the feedback law (36) and the adaptation laws (39) and (41), one obtains that

$$\dot{V} \leq -\tfrac{1}{2}\mathbf{e}^TR\mathbf{e} < 0, \tag{48}$$

and $(G^{*\mathrm{n}} + Y_G\hat{\Theta}_G)$ will not lose rank, if we choose the initial parameter guess $\hat{\Theta}_{Gi}(0)$ inside the set $\Omega_{\Theta_{Gi}}$. For instance, we may take $\hat{\Theta}_{Gi}(0) = 0$. Moreover, Eq. (48) implies that $\mathbf{e} \to 0$ as $t \to \infty$, since $R$ is positive-definite.

## IV. Numerical Example

A numerical example for a satellite with a VSCMGs cluster is provided in this section to test the proposed adaptive control algorithm. In the previous section, the simplified equations of motion, given by (5), with several assumptions were used for the adaptive control design, but in this section the complete nonlinear equations of motion, given in Eq.(1), and the acceleration steering law derived in Ref. 8 are used to predict and validate the performance of the proposed controllers under realistic conditions. The parameters used for the simulations are chosen as in Table 1. We also assume a standard four-VSCMG pyramid configuration, as shown in Figure 3.

**Table 1. Simulation Parameters**

| Symbol | Value | Units |
|---|---|---|
| $N$ | 4 | – |
| $\theta$ | 54.75 | deg |
| $\boldsymbol{\omega}(0)$ | $[0,0,0]^T$ | rad/sec |
| $\dot{\boldsymbol{\omega}}(0)$ | $[0,0,0]^T$ | rad/sec$^2$ |
| $\boldsymbol{\sigma}(0)$ | $[0,0,0]^T$ | – |
| $\boldsymbol{\gamma}(0)$ | $[0,0,0,0]^T$ | rad |
| $\dot{\boldsymbol{\gamma}}(0)$ | $[0,0,0,0]^T$ | rad/sec$^2$ |
| ${}^BI$ | $\begin{bmatrix} 15053 & 3000 & -1000 \\ 3000 & 6510 & 2000 \\ -1000 & 2000 & 11122 \end{bmatrix}$ | kg m$^2$ |
| $I_{\rm cg}$ | diag{0.7, 0.7, 0.7, 0.7} | kg m$^2$ |
| $I_{\rm wt}, I_{\rm wg}$ | diag{0.4, 0.4, 0.4, 0.4} | kg m$^2$ |
| $I_{\rm gs}, I_{\rm gt}, I_{\rm gg}$ | diag{0.1, 0.1, 0.1, 0.1} | kg m$^2$ |

The nominal values of the axis directions at $\boldsymbol{\gamma} = [0,0,0,0]^T$ in this pyramid configuration are

$$A_{s0}^{\rm n} = [\mathbf{s}_1, \mathbf{s}_2, \mathbf{s}_3, \mathbf{s}_4] = \begin{bmatrix} 0 & -1 & 0 & 1 \\ 1 & 0 & -1 & 0 \\ 0 & 0 & 0 & 0 \end{bmatrix}, \tag{49}$$

$$A_{t0}^{\rm n} = [\mathbf{t}_1, \mathbf{t}_2, \mathbf{t}_3, \mathbf{t}_4] = \begin{bmatrix} -0.5774 & 0 & 0.5774 & 0 \\ 0 & -0.5774 & 0 & 0.5774 \\ 0.8165 & 0.8165 & 0.8165 & 0.8165 \end{bmatrix}. \tag{50}$$

The (unknown) actual axis directions used in the present example are assumed as*

$$A_{s0} = \begin{bmatrix} 0.0745 & -0.9932 & -0.1221 & 0.9901 \\ 0.9919 & -0.1024 & -0.9911 & -0.1033 \\ 0.1033 & -0.0547 & -0.0536 & -0.0954 \end{bmatrix}, \tag{51}$$

$$A_{t0} = \begin{bmatrix} -0.6570 & 0.0029 & 0.6485 & 0.1394 \\ -0.0291 & -0.4929 & -0.1206 & 0.6335 \\ 0.7533 & 0.8701 & 0.7516 & 0.7611 \end{bmatrix}. \tag{52}$$

The reference trajectory is chosen so that the initial reference attitude is aligned with the actual attitude, and the angular velocity of the reference attitude is chosen as

$$\omega_d(t) = 0.02 \times \Big(\sin(2\pi t/800),\ \ \sin(2\pi t/600),\ \ \sin(2\pi t/400)\Big)^T \text{rad/sec}. \tag{53}$$

Figure 4 shows the time history of the reference attitude using the Euler parameters (quaternions).

The feedback gain $K$ in (31) is chosen so that the eigenvalues of the matrix $A = A_0 - BK$ are given by

$$\text{eig}(A) = \{-0.1 \pm 0.1i,\ -0.1\sqrt{2}, -0.15 \pm 0.15i,\ -0.15\sqrt{2}\}.$$

The remaining design parameters for the adaptive control law are chosen as

$$R = \mathbf{I}_6, \quad \beta_{Gi} = 0.1, \quad \delta_{Gi} = 0.05, \quad \alpha_F = 1.0 \times 10^7, \quad \alpha_G = 1.0 \times 10^3.$$

*The actual directions are taken by small angle rotations from the nominal directions, thus the orthogonality $\hat{\mathbf{t}}_i \cdot \hat{\mathbf{s}}_i = 0$ still holds for each VSCMG.

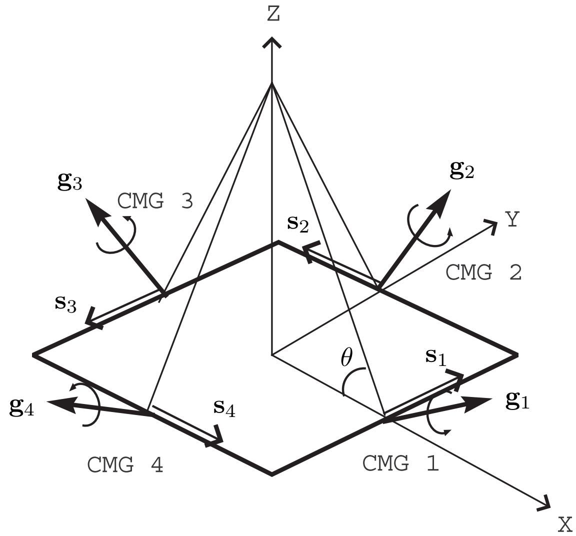


**Figure 3. A VSCMGs system with pyramid configuration at $\boldsymbol{\gamma} = [0, 0, 0, 0]^T$.**

Before applying the designed adaptive control law, we first performed a simulation without adaptation, for comparison purposes. Figure 5 shows the attitude error under the control law with the adaptation gains $\alpha_F$ and $\alpha_G$ set to zero.

Figures 6-9 show the simulation results using the designed adaptive control law. As shown in Figure 6, the attitude error is significantly attenuated using the adaptive controller. The error does not converge to zero because of the simplifying assumption made during the design step of the adaptation law, when the effects of extra (albeit small) dynamics were ignored. Figure 7 shows the time history of the parameter estimate $\hat{\Theta}_F$. The bold dot horizontal lines denote the actual values of the components of $\Theta_F$. The estimates approach the actual values, but they do not perfectly converge to these values owing again to the ignored dynamics. Figure 8 shows the time history of $\|\hat{\Theta}_{Gi}\|^2$. It is shown that $\|\hat{\Theta}_{Gi}\|^2$ does not drift more than $\beta_{Gi} + \delta_{Gi} = 0.15$ owing to the smooth projection algorithm.

As is the case with similar adaptive algorithms, the designed adaptive law does not guarantee a priori that the parameter estimates converge to their actual values. This is because the number of the parameters to be estimated is large. Note that, generally speaking – and for a linear system – convergent estimation of $m$ parameters requires at least $m/2$ sinusoids in the reference signal. For the nonlinear case such simple relation may not be valid.[25] Additionally, in Figures 7 and 8, irregular large excursions of the parameter estimates (where the parameter estimates exhibit intermittent short periods of burst), are shown. These phenomena are well known in the adaptive control literature and they generally occur due to lack of persistency of excitation.[26] Finally, Figure 9 shows the states of the VSCMG cluster. The values remain within their acceptable limits.

# V. Conclusion

An adaptive control law is proposed for the attitude control problem of a spacecraft with a flywheel actuator model having unknown bounded constant uncertainties. The general case of a spacecraft with a variable-speed CMG (VSCMG) cluster is dealt with in detail. The standard CMG and RW actuators follow our developments as special cases. The adaptive law is based on the smooth projection algorithm in order to avoid singularities that may be caused by the drift of the parameter estimates. The projection algorithm forces the parameter estimates to stay inside a certain convex set that contains the unknown actual values. Although the control law was designed based on the simplified equations of motion, numerical examples using the full equations showed very good performance, with the tracking error significantly reduced when compared to the non-adaptive case. Though the method still leaves room for improvement (for instance, a way to reduce the number estimated parameters would be extremely beneficial), the present article provides

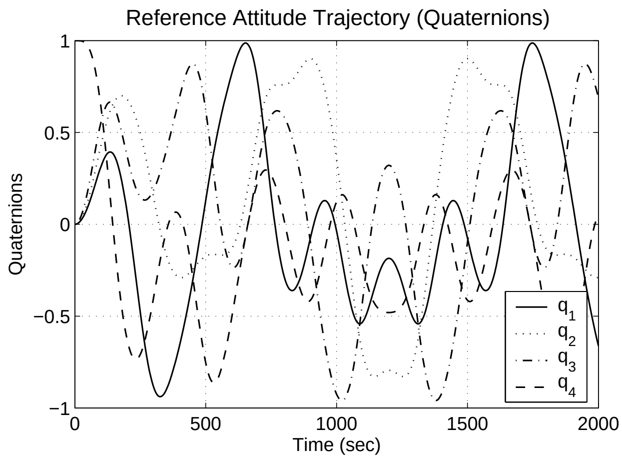


**Figure 4. The Reference Attitude Trajectory.**

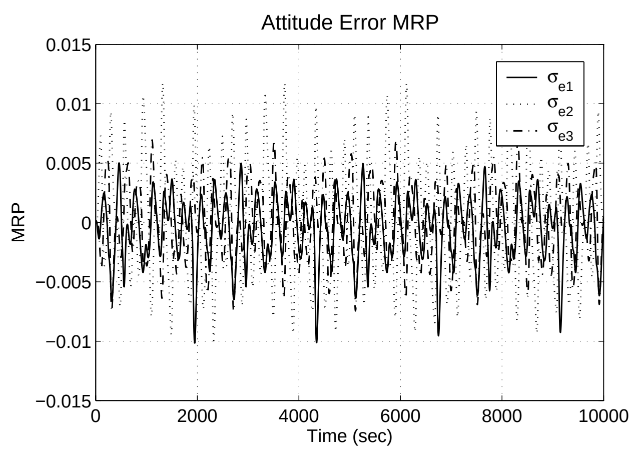


**Figure 5. The Attitude Error Trajectory Without Adaptation.**

a first step in solving the general problem of spacecraft control with actuator misalignment/uncertainties. This problem does not seem to have received its due attention in the literature.

## References


[1]Slotine, J. J. E. and Benedetto, M. D. D., "Hamiltonian Adaptive Control of Spacecraft," *IEEE Transactions on Automatic Control*, Vol. 35, No. 7, July 1990, pp. 848–852.

[2]Bishop, R., Paynter, S., and Sunkel, J., "Adaptive Control of Space Station with Control Moment Gyros," *IEEE Control Systems Magazine*, Vol. 12, Oct.1992, pp. 23–28.

[3]Sheen, J. and Bishop, R., "Adaptive Nonlinear Control of Spacecraft," *American Control Conference*, Baltimore, Maryland, 1994, pp. 2867–2871.

[4]Zaremba, A., "An Adaptive Scheme with Parameter Identification for Spacecraft Attitude Control," *Proceedings of American Control Conference*, 1997, pp. 552–556.

[5]Ahmed, J. and Bernstein, D., "Adaptive Control of a Dual-Axis CMG with an Unbalanced Rotor," *Proceedings of the 37th IEEE Conference on Decision and Control*, Tampa, FL, Dec.1992, pp. 4531–4536.

[6]Ahmed, J., Coppola, V., and Bernstein, D., "Adaptive Asymptotic Tracking of Spacecraft Attitude Motion with Inertia Matrix Identification," *Journal of Guidance, Control, and Dynamics*, Vol. 21, No. 5, 1998, pp. 684–691.

[7]Schaub, H., Akella, M. R., and Junkins, J. L., "Adaptive Realization of Linear Closed-Loop Tracking Dynamics in the Presence of Large System Model Errors," *Journal of the Astronautical Sciences*, Vol. 48, No. 4, Oct.-Dec. 2000, pp. 537–551.

[8]Yoon, H. and Tsiotras, P., "Spacecraft Adaptive Attitude And Power Tracking With Variable Speed Control Moment Gyroscopes," *Journal of Guidance, Control, and Dynamics*, Vol. 25, No. 6, Nov.-Dec. 2002, pp. 1081–1090.

[9]Tsiotras, P., Shen, H., and Hall, C., "Satellite Attitude Control and Power Tracking with Energy/Momentum Wheels,"

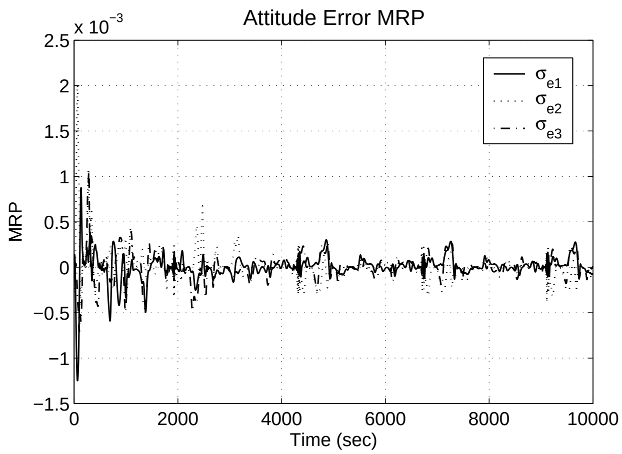


**Figure 6. The Attitude Error Trajectory With Adaptation.**

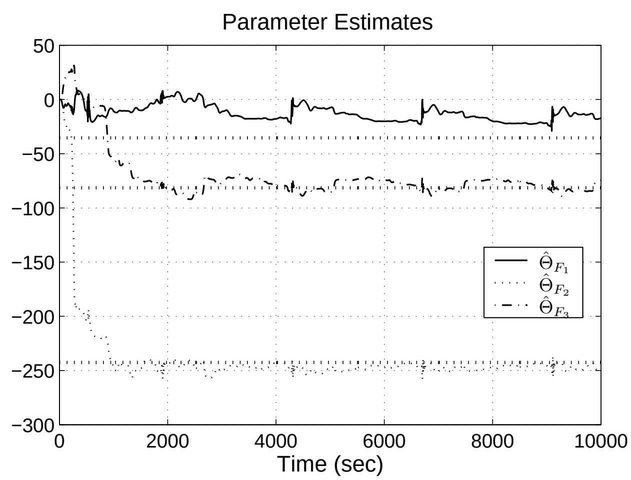


**Figure 7. Parameter Estimate $\hat{\Theta}_F$.**

*Journal of Guidance, Control, and Dynamics*, Vol. 24, No. 1, 2001, pp. 23–34.

[10]Yoon, H. and Tsiotras, P., "Singularity Analysis of Variable-Speed Control Moment Gyros," *Jornal of Guidance, Control, and Dynamics*, Vol. 27, No. 3, 2004, pp. 374–386.

[11]Slotine, J.-J. E. and Li, W., "Adaptive Manipulator Control : A Case Study," *IEEE Transactions on Automatic Control*, Vol. 33, No. 11, Nov. 1988, pp. 995 – 1003.

[12]Ge, S. S., "Adaptive Control of Robots Having Both Dynamical Parameter Uncertainties and Unknown Input Scalings," *Mechatronics*, Vol. 6, No. 5, 1996, pp. 557–569.

[13]Chang, Y.-C., "An Adaptive $\mathcal{H}_\infty$ Tracking Control for a Class of Nonlinear Multiple-Input-Multiple-Output (MIMO) Systems," *IEEE Transactions on Automatic Control*, Vol. 46, No. 9, Sep. 2001, pp. 1432–1437.

[14]Pomet, J.-B. and Praly, L., "Adaptive Nonlinear Regulation : Estimation from the Lyapunov Equation," *IEEE Transactions on Automatic Control*, Vol. 37, No. 6, June 1992, pp. 729–740.

[15]Khalil, H. K., *Nonlinear Systems*, Prentice Hall, New Jersey, 2nd ed., 1996.

[16]Schaub, H., Vadali, S. R., and Junkins, J. L., "Feedback Control Law for Variable Speed Control Moment Gyroscopes," *Journal of the Astronautical Sciences*, Vol. 46, No. 3, 1998, pp. 307–328.

[17]Richie, D., Tsiotras, P., and Fausz, J., "Simultaneous Attitude Control and Energy Storage Using VSCMGs: Theory and Simulation," *Proceedings of the American Control Conference*, June 25-27, 2001, pp. 3973–3979, Arlington, VA.

[18]Yoon, H., *Spacecraft Attitude and Power Control Using Variable Speed Control Moment Gyros*, Ph.D. thesis, Georgia Institute of Technology, Atlanta, GA., December 2004.

[19]Ford, K. A. and Hall, C. D., "Flexible Spacecraft Reorientations Using Gimbaled Momentum Wheels," *Advances in the Astronautical Sciences, Astrodynamics*, edited by F. Hoots, B. Kaufman, P. J. Cefola, and D. B. Spencer, Vol. 97, Univelt, San Diego, 1997, pp. 1895–1914.

[20]Richie, D. J., Tsiotras, P., and Fausz, J. L., "Simultaneous Attitude Control and Energy Storage using VSCMGs : Theory and Simulation," *Proceedings of American Control Conference*, 2001, pp. 3973–3979.

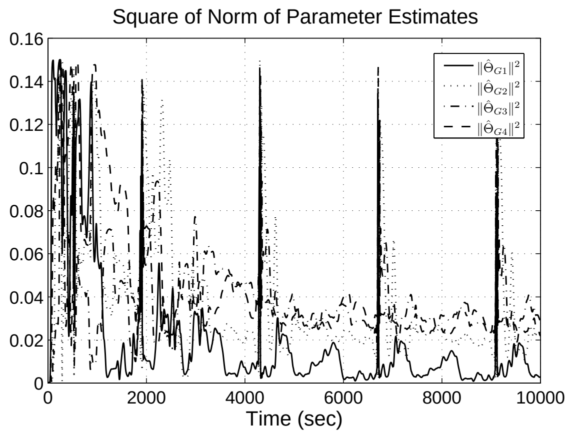


(a) $i = 1, 2, 3, 4$

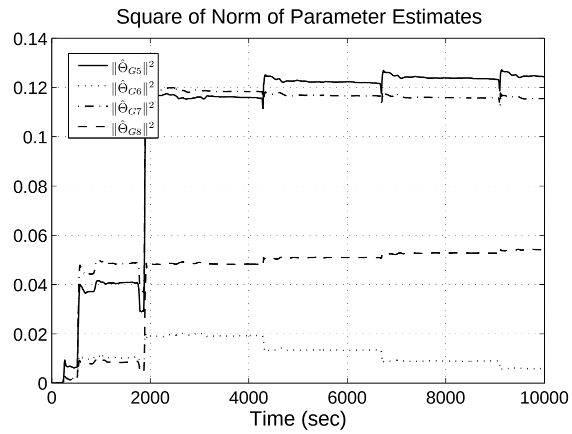


(b) $i = 5, 6, 7, 8$

**Figure 8. Square of Norms of Parameter Estimate $\|\hat{\Theta}_{Gi}\|^2$.**

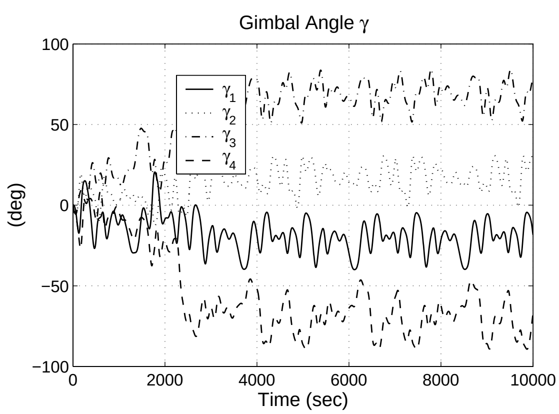


(a) Gimbal angle $\boldsymbol{\gamma}$

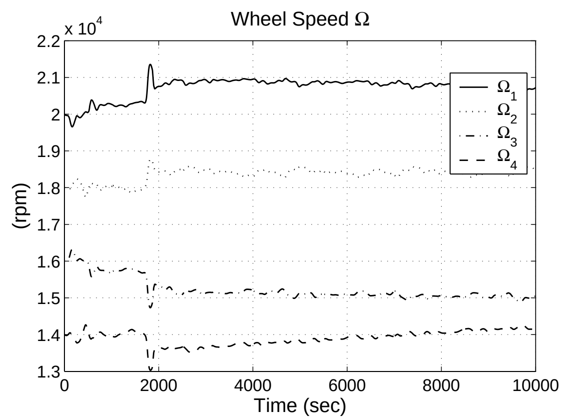


(b) Wheel Speed $\boldsymbol{\Omega}$

**Figure 9. Gimbal Angle $\boldsymbol{\gamma}$ and Wheel Speed $\boldsymbol{\Omega}$.**


[21] Tsiotras, P., "Stabilization and Optimality Results for the Attitude Control Problem," *Journal of Guidance, Control, and Dynamics*, Vol. 19, No. 4, 1996, pp. 772–779.

[22] Schaub, H. and Junkins, J. L., "Stereographic Orientation Parameters for Attitude Dynamics: A Generalization of the Rodrigues Parameters," *Journal of the Astronautical Sciences*, Vol. 44, No. 1, 1996, pp. 1–19.

[23] Shuster, M. D., "A Survey of Attitude Representations," *Journal of the Astronautical Sciences*, Vol. 41, No. 4, 1993, pp. 439–517.

[24] Tsiotras, P., Junkins, J. L., and Schaub, H., "Higher Order Cayley-Transforms with Applications to Attitude Representations," *Journal of Guidance, Control, and Dynamics*, Vol. 20, No. 3, 1997, pp. 528–534.

[25] Slotine, J. and Li, W., *Applied Nonlinear Control*, Prentice Hall, New Jersey, 1991.

[26] Anderson, B. D. O., "Adaptive Systems, Lack of Persistency of Excitation and the Bursting Phenomenon," *Automatica*, Vol. 21, 1985, pp. 247–258.